Inferring extinction date of a species using non-homogeneous Poisson processes with a change-point

Saritha Kodikara[1], Haydar Demirhan[1], Yan Wang[1], and Lewi Stone[1,2]

[1]School of Science, Mathematical Sciences, RMIT University, Melbourne, Australia. Email:sarithakalhari.kodikara@rmit.edu.au

[2]Biomathematics Unit, School of Zoology, Faculty of Life Science, Tel-Aviv University, Israel.

This is the pre-peer reviewed version of the following article: (Kodikara *et al.* 2020), which has been published in final form at https://doi.org/10.1111/2041-210X.13542. This article may be used for non-commercial purposes in accordance with Wiley Terms and Conditions for Use of Self-Archived Versions.

Abstract

1. Bayesian methods have been developed for inferring the true year of extinction of a species from sighting records that have both certain and uncertain sightings. These methods typically make the restrictive assumption that all sighting types (i.e. certain, valid uncertain, invalid uncertain) derive from independent homogeneous Poisson processes.
2. In this study, the constant rate assumption in the homogeneous Poisson process is relaxed by allowing certain and uncertain sightings to follow independent non-homogeneous Poisson processes. The model can thus identify whether or not any of the sighting rates were increasing, decreasing or constant. In addition, a change-point is introduced to model the uncertain sightings, where the sighting rates before and after the change-point vary.
3. We have used Markov Chain Monte Carlo (MCMC) sampling to generate the posterior distributions for model parameters including species extinction time. The proposed method was applied to the sighting records of the black-footed ferret (*Mustela nigripes*) and the Ivory-billed Woodpecker (IBW; *Campephilus*

principalis) species.

4. Based on a hypothesis test, the results of the model indicate that the species both species have gone extinct and the time this occurred is inferred. Moreover, a decline in the certain sighting rate was also inferred for both these species, possibly indicating the decrease in the species abundance as it converges to extinction. Thus, earlier model that assumes a constant sighting rate may well be biased. Uncertain sightings rates for the IBW were found to increase before extinction (indicating possibly some additional ecological attention received near extinction) and remained constant after extinction.

Keywords: Non-homogeneous Poisson processes, Bayesian modeling, Extinction year, Sighting record, Uncertain sightings, change-point

1 Introduction

Continued ongoing loss of global biodiversity is one of the most pressing contemporary ecological problems that threatens valuable ecosystem services and human well-being (Ceballos *et al.* 2010; Dirzo & Raven 2003; Mace *et al.* 2012; Daily & Matson 2008; Ehrlich & Ehrlich 2013; Barnosky *et al.* 2011). Theoretical ecologists have therefore taken great interest in studying processes that lead to species extinctions, from complex spatio-temporal models to dealing with methods that infer from empirical data that predict whether a species has become extinct or not. It is the latter methods that will be of concern to us here. The date of extinction, or the time of the disappearance of the last individual of a species, is rarely observed and even harder to detect. Therefore, where-ever possible, any inference concerning the extinction of a species should be based on a variety of information sources. This includes time series of historical sightings (i.e. sighting records), the effort expended in searching for the species, change in abundance over time (i.e. population trajectories), potential remaining habitat and its relationship to abundance, the severity and extent of processes threatening species, and intrinsic taxon information (e.g. life-history traits) (Boakes *et al.* 2015). Ideally, we would like to use all of this information when attempting to infer whether a species has gone extinct or not. However, in reality the only available data is often just restricted to time series of sightings.

Sighting history provides fundamental knowledge about a species existence and also the possibility of its extinction. However, extinction becomes a certainty only when there are no surviving individuals of the species, which is generally difficult or impossible to ascertain. Thus the assessment of extinction can benefit from the development of probabilistic frameworks (Elphick *et al.* 2010). A number of studies have developed methods to calculate an

extinction probability based on the record of sightings of a species through time. A sighting record typically contains mixed-certainty sightings, some being certain and others uncertain. For example, observing an actual specimen of a species would be classified as a certain sighting, while an ambiguous photograph would be classified as an uncertain sighting. Thus, predicting the probability of a species being extinct from a sighting record ideally requires allowing for both certain and uncertain sightings.

Working with uncertain sightings requires further terminology. While certain sightings may confidently be considered always "valid", uncertain sightings are either "valid" or "invalid", given we are not sure whether we have identified the species correctly or not. In practice, it is impossible to know which of the uncertain sightings are valid and actually real, and which are invalid and thus errors. The most straightforward approach when modeling both these sighting types is to assume that the sighting rate of a species over time is constant for each sighting type, i.e., for all certain, for all valid uncertain and for all invalid uncertain sightings (Solow *et al.* 2012; Solow & Beet 2014; Lee *et al.* 2014; 2017). However, this constant sighting rate assumption is often not always a realistic assumption, and this motivated Solow (1993)'s test for extinction in a declining population. In this approach, sightings were modelled as a non-stationary Poisson process with an exponentially declining rate function. But the method was only formulated for dealing with sighting records having only certain sightings, and which appear to have a decline in the sighting rate.

In this paper, we extend the work of Solow & Beet (2014) to develop a more general Bayesian framework to infer the extinction year by relaxing the assumption of a constant sighting rate. The new model assumes that the sightings follow a non-homogeneous Poisson process that has an intensity function of Weibull hazard form, and often referred to as a Weibull process, or more commonly, a power-law process (Rigdon & Basu 1989; Ho 1991; Rao *et al.* 2006).Our new approach can detect if the sighting rate (certain/uncertain) is constant, decreasing or increasing over the study period. It is important to have this flexibility in an extinction model because, for example, the certain sighting rate can decline before extinction due to declining abundance, or the uncertain sighting rate can increase due to significant attention from the media. In this paper, it is assumed that the time of extinction can be viewed as a change-point for the uncertain sightings. Hence, the rate of uncertain sightings can be decreasing, increasing or constant after extinction regardless of their behaviour before extinction.

2 Model Development

Let $N(t) \geq 0$ be the total number of sightings in the time interval $[0, t)$, $t \geq 0$. Then, assuming that $(N = \{N(t) : t \geq 0\})$ evolves according to a non-homogeneous Poisson processes with rate given by $\lambda(t)$, the mean of the process is given by:

$$E\Big(N(t)\Big) = m(t) = \int_0^t \lambda(s) \quad ds. \tag{1}$$

By the properties of the Poisson distribution, the probability of k sightings between time t and $(t + s)$ is given by:

$$\begin{aligned} P(N(t+s) - N(t) = k) &= \frac{[\int_t^{t+s} \lambda(s)ds]^k}{k!} \exp\{-\int_t^{t+s} \lambda(s)ds\} \\ &= \frac{[m(t+s) - m(t)]^k}{k!} \exp\{-[m(t+s) - m(t)]\}. \end{aligned} \tag{2}$$

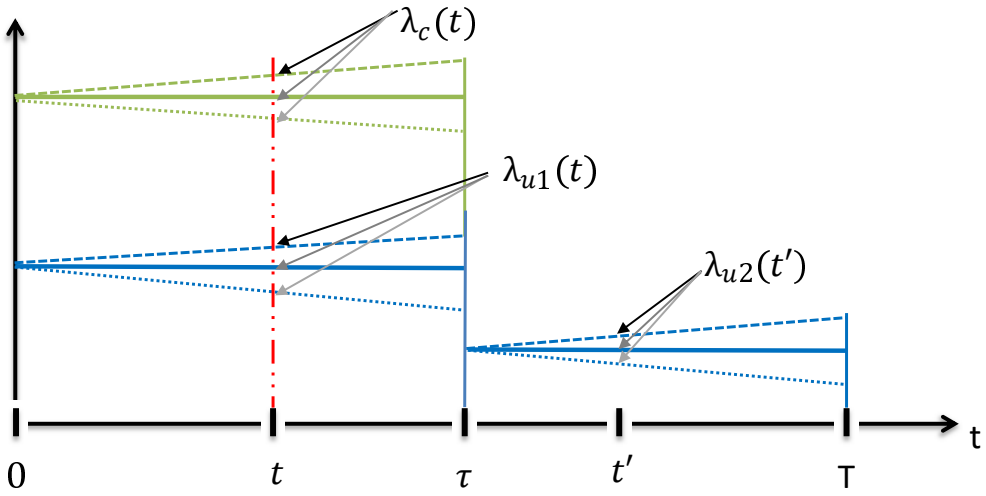

Figure 1: Certain sightings can evolve according to a homogeneous or non-homogeneous Poisson process with rate given by $\lambda_c(t)$. Uncertain sightings can also evolve according to a Poisson process but with the presence of a change-point τ_E. The rate of the uncertain sightings can either be $\lambda_{u1}(t)$ or $\lambda_{u2}(t)$ depending on whether t is before or after extinction. The solid line indicates the homogeneous Poisson process, while the dashed (i.e. increasing rate) and dotted (i.e. decreasing rate) horizontal lines indicate two different non-homogeneous Poisson processes. Whether these non-homogeneous Poisson rates behave in a linear or non-linear pattern depends on the rate function used.

For a sighting record, let $N_c(t) \geq 0$ and $N_u(t) \geq 0$ be the number of certain sightings and uncertain sightings in the time interval $[0, t)$, $t \geq 0$. We assume that the number of certain sightings ($N_c = \{N_c(t) : t \geq 0\}$) evolves according to a non-homogeneous Poisson process with rate given by $\lambda_c(t)$ in the interval 0 to τ_E, where τ_E is the time of extinction. While the certain sightings must stop after the extinction time τ_E, the invalid uncertain sightings should continue after extinction. The extinction time (τ_E) can be considered as a change-point for uncertain sightings because before τ_E the uncertain sightings consists of both valid and invalid uncertain sightings, but after τ_E there are only invalid uncertain sightings. Hence the uncertain sightings are assumed to evolve according to a non-homogeneous Poisson processes with the presence of the change-point $\tau_E \in (0, \infty)$. Before extinction, the rate of uncertain sighting is $\lambda_{u1}(t)$, but this changes to $\lambda_{u2}(t)$ after τ_E (see Fig. 1).

In the present case, the rate of certain sighting $\lambda_c(t)$ is defined as follows:

$$\lambda_c(t) = (\alpha_c/\sigma_c)(t/\sigma_c)^{\alpha_c - 1}, \quad t \leq \tau_E. \tag{3}$$

The rate for uncertain sightings $\lambda_u(t)$ is defined as follows with a change-point at τ_E:

$$\lambda_u(t) = \begin{cases} \lambda_{u1}(t) = (\alpha_{u1}/\sigma_{u1})(t/\sigma_{u1})^{\alpha_{u1} - 1}, & t \leq \tau_E \\ \lambda_{u2}(t) = (\alpha_{u2}/\sigma_{u2})(t/\sigma_{u2})^{\alpha_{u2} - 1}, & t > \tau_E. \end{cases} \tag{4}$$

The rates of certain and uncertain sightings in Equations 3 and 4 are assumed to be of the Weibull hazard function form, i.e., $(\alpha/\sigma)(t/\sigma)^{\alpha-1}$, where σ and α are the scale and shape parameters respectively. The Weibull rate function is a very flexible function that can be adjusted to mimic real-world sighting rate behaviours, using its scale (σ) and shape (α) parameters. For example, a Weibull shape parameter value less than one mimics a decreasing sighting rate over time, while a value greater than one mimics an increasing sighting rate. Because of the flexible shape and its ability to model a wide range of rates, the Weibull rate function is adopted in this chapter to model the sighting rates. Also, the Weibull distribution can be derived theoretically as a form of Extreme Value Distribution. This may explain why it has been used in the literature to model the k most recent sighting times of a species, ordered from most recent sighting time to least recent sighting time (i.e $T_1 > T_2 > ... > T_k$) (Smith & Weissman 1985; Hall *et al.* 1999; Roberts & Solow 2003; Solow 2005).

The mean certain and uncertain sighting rates, which change with time, can be obtained

using Equation 1 as:

$$m_c(t) = (t/\sigma_c)^{\alpha_c}, t \leq \tau_E. \tag{5}$$

$$m_u(t) = \begin{cases} m_{u1}(t) = (t/\sigma_{u1})^{\alpha_{u1}}, & t \leq \tau_E \\ m_{u1}(\tau_E) + m_{u2}(t) - m_{u2}(\tau_E) & \\ \quad = (\tau_E/\sigma_{u1})^{\alpha_{u1}} + (t/\sigma_{u2})^{\alpha_{u2}} - (\tau_E/\sigma_{u2})^{\alpha_{u2}}, & t > \tau_E. \end{cases} \tag{6}$$

Here $\tau_E > 0$ is the extinction time and $\theta = (\alpha_c, \alpha_{u1}, \alpha_{u2}, \sigma_c, \sigma_{u1}, \sigma_{u2}, \tau_E)$ is the vector of parameters of the model, where α_* and σ_* refers to the shape and scale parameters of the Weibull distribution. Here, '$*$' refers to either the certain sightings (c) or the uncertain sightings before extinction (u1) or the uncertain sightings after extinction (u2). In this work, we assume that these parameters are random variables that need to be estimated.

In what follows, we will be interested in determining α_* in Equations 5 and 6 as it reflects whether the sighting rate was increasing, decreasing or constant. Based on the value of α_* the sighting rate $\lambda_*(t)$ can be classified as follows using the rate functions given in Equations 3 and 4.

$$\lambda_*(t) = \begin{cases} \text{decreasing}, & \text{if } \alpha_* < 1 \\ \text{constant}, & \text{if } \alpha_* = 1 \\ \text{increasing}, & \text{if } \alpha_* > 1 \end{cases} \tag{7}$$

Now we discuss the development of the likelihood and show how the likelihood and prior specification is used to obtain the posterior distribution of θ i.e., the vector containing all parameters including τ_E the extinction time. Let $T > 0$, $K_c > 0$ and $K_u > 0$ be fixed integers. Assume that there are K_c certain sightings in the time interval $[0, \tau_E)$ and K_u uncertain sightings in the time interval $[0, T)$. Then, let $K_u(\tau_E)$ be the number of uncertain sightings prior to extinction time τ_E. $D_c = \{y_{c_1}, y_{c_2}, ..., y_{K_c}\}$ and $D_u = \{y_{u_1}, y_{u_2}, ..., y_{K_u}\}$ denote the two types of observed sightings, certain and uncertain, while y_i indicate the time of the sighting. Then using the likelihood function and the prior distributions, the posterior

distribution of the parameters of interest can be expressed as:

$$P(\theta|D_c, D_u) \propto L(D_c, D_u|\theta)P(\theta), \tag{8}$$

where $P(\theta|D_c, D_u)$ is the posterior distribution of θ given the data D_c, D_u; $P(\theta)$ represents all the prior distributions for model parameters; and $L(D_c, D_u|\theta)$ is the likelihood function of the model.

To build the full likelihood, we use the result that the likelihood of sighting times $D = \{y_1, y_2, ..., y_K\}$ arising from a non-homogeneous Poisson process with rate $\lambda(t)$ over the period $[0, T)$ is $\prod_{i=1}^{K} \lambda(y_i|\theta) \exp[-m(T|\theta)]$. Thus, the full likelihood with the presence of a change-point takes the following form (see, for instance, Achcar *et al.* (2010); Guarnaccia *et al.* (2015)):

$$\begin{aligned}
&L(D_c, D_u|\theta) \\
&= L(D_c|\theta) \times L(D_u|\theta) \\
&= \Big[\prod_{i=1}^{K_c} \lambda_c(y_{c_i}|\theta) \exp[-m_c(\tau_E|\theta)]\Big] \times \Big[\prod_{j=1}^{K_u(\tau_E)} \lambda_{u1}(y_{u_j}|\theta) \exp[-m_{u1}(\tau_E|\theta)]\Big] \\
&\quad \times \Big[\prod_{j=K_u(\tau_E)}^{K_u} \lambda_{u2}(y_{u_j}|\theta) \exp[-(m_{u2}(T|\theta) - m_{u2}(\tau_E|\theta))]\Big] \\
&\propto \Big[\Big(\frac{\alpha_c}{\sigma_c^{\alpha_c}}\Big)^{K_c} \prod_{i=1}^{K_c} (y_{ci}^{\alpha_c - 1}) \exp[-(\tau_E/\sigma_c)^{\alpha_c}]\Big] \\
&\quad \times \Big[\Big(\frac{\alpha_{u1}}{\sigma_{u1}^{\alpha_{u1}}}\Big)^{K_u(\tau_E)} \prod_{j=1}^{K_u(\tau_E)} (y_{u_j}^{\alpha_{u1} - 1}) \exp[-(\tau_E/\sigma_{u1})^{\alpha_{u1}}]\Big] \\
&\quad \times \Big[\Big(\frac{\alpha_{u2}}{\sigma_{u2}^{\alpha_{u2}}}\Big)^{K_u - K_u(\tau_E)} \prod_{j=K_u(\tau_E)}^{K_u} (y_{u_j}^{\alpha_{u2} - 1}) \exp[-((T/\sigma_{u2})^{\alpha_{u2}} - (\tau_E/\sigma_{u2})^{\alpha_{u2}})]\Big]
\end{aligned} \tag{9}$$

where $K_u(\tau_E)$ is the number of uncertain sightings prior to extinction time (τ_E).

If there are only certain sightings, then the likelihood in Equation 9 can be significantly

simplified into Equation 10, by setting $L(D_u|\theta) = 1$.

$$\begin{aligned} L(D_c|\theta) &= \Big[\prod_{i=1}^{K_c} \lambda_c(y_{c_i}|\theta)\exp[-m_c(\tau_E|\theta)]\Big] \\ &\propto \Big[\Big(\frac{\alpha_c}{\sigma_c^{\alpha_c}}\Big)^{K_c}\prod_{i=1}^{K_c}(y_{c_i}^{\alpha_c-1})\exp[-(\tau_E/\sigma_c)^{\alpha_c}]\Big] \end{aligned} \tag{10}$$

Accordingly, the posterior distributions can be obtained using Equation 8 along with the same prior distributions defined earlier for α_c, σ_c and τ_E. Similar modification can be made to arrive at a model that does not assume a change-point for uncertain sightings by fitting a single non-homogeneous Poisson process for the uncertain sightings (i.e. $\lambda_{u2} = \lambda_{u1}$). In such a situation, the uncertain sightings are independent of the extinction time. Thus, inclusion of uncertain sightings does not provide additional information about extinction. However, for species sighting data, the change-point assumption is important since it is possible to have both valid and invalid uncertain sightings prior to extinction, but only invalid ones afterwards.

For the study that follows, the prior distributions for shape (α_c, α_{u1} and α_{u2}) and scale (σ_c, σ_{u1} and σ_{u2}) parameters are chosen to be non-informative Uniform distributions, i.e. Unif(0, 1000), giving the sighting rates a vague behaviour. However, if there is prior knowledge about the sighting rates, the prior distributions can be modified accordingly. Following previous Bayesian approaches in the literature (Solow *et al.* 2012; Solow & Beet 2014), the prior distribution for τ_E is chosen to be an exponential distribution:

$$p(\tau_E|\gamma) = \gamma\exp(-\gamma\tau_E) \tag{11}$$

In order to use a weakly informative prior for τ_E, the rate parameter γ in Equation 11 is chosen as 0.005 in the exponential distribution. This prior specification reflects an expected extinction time to be 200 years with a variance of 40,000 years. Along with these priors and likelihood function defined in Equation 9, we obtain posterior distributions for model parameters including, most importantly τ_E, via the Markov Chain Monte Carlo (MCMC) algorithm using Equation 8. In addition to τ_E the extinction time, the posterior distribution of the parameter α is of particular interest, as it reflects whether the sightings were increasing, decreasing or constant.

In the MCMC implementation, we generated 4 chains each with 10,000 thinned iterations for the black-footed ferret and for the Ivory-billed woodpecker. Compared to the Ivory-billed woodpecker, the black-footed ferret sighting record resulted in highly auto-correlated MCMC chains. Thus, a thinning value of 360 and 13 were used to reduce the auto-correlation in chains for the black-footed ferret and Ivory-billed woodpecker, respectively. These numbers were obtained by going through a trial and error process to obtain less auto-correlated chains. MCMC diagnostic checks were carried out in respect to convergence, auto-correlation and effective sample size and no indication of any problem for any parameter (e.g. τ_E, α_c, σ_c etc.) was observed. Detailed descriptions on the diagnostics are not discussed here as it is out of the scope of this paper. However, such details can be found in the supplementary materials of our recent paper (Kodikara *et al.* 2020).

3 Results

In this section the model outlined above is first applied to a simple example with only certain sightings using the data collected for the black-footed ferret. This is then followed by the example of the Ivory-billed woodpecker (IBW) where both certain and uncertain sightings are included in the modeling approach.

3.1 Black-footed ferret

The black-footed ferret *(Mustela nigripes)*, found in the State of Wyoming, USA, was once thought to be extinct, but it was successfully reintroduced back into the wild after captive propagation (Dobson & Lyles 2000; Wisely *et al.* 2008). Before this reintroduction, Solow (1993) used the sightings of the black-footed ferret as a method for testing extinction in declining populations. The sighting record consists of 28 certain sightings over the period January 1972 to December 1990 (Solow 1993). Even though the black-footed ferret was reintroduced back into the wild, the sightings published in Solow (1993) are useful for studying extinction in a declining population (Jarić & Ebenhard 2010).

The posterior distribution of the extinction time τ_E is plotted in Figure 2a and the 95% Highest Density Interval (HDI) for the posterior extinction year is given in Table 1. In these calculations, as similar to Solow (1993), the time unit was taken to be a month. According to Table 1, the median extinction year is 1985 for the black-footed ferret. The 95% HDI upper bound for τ_E was found to be 1987 and hence we could infer that the species is highly likely to be extinct by the sighting end period (i.e. December 1990). This inference agrees with the finding of Solow (1993), where his method provides moderately strong evidence against the existence of the black-footed ferret. In addition, the posterior distribution for parameter α_c has a 95% HDI between 0.45 and 1 indicating that the certain sightings have a

high tendency to decline from the beginning of the observation period as suspected by Solow (1993).

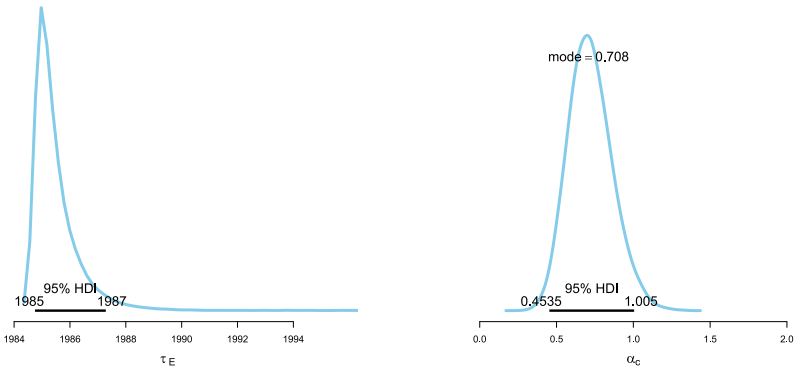

(a) (b)

Figure 2: Posterior distribution plots for the model parameters τ_E and α_c for black-footed ferret. Black solid line above x-axis shows the 95% HDI for the posterior distribution. (a) Posterior distribution of τ_E. (b) Posterior distribution of α_c.

Table 1: Summary of the posterior distributions of τ_E and α_c for the black-footed ferret

	95% HDI Low	median	95% HDI High
$\tau_E \vert S$	1984.75	1985.23	1987.28
$\alpha_c \vert S$	0.45	0.71	1.01

3.2 Ivory-billed woodpecker

The Ivory-Billed Woodpecker (IBW; *Campephilus principalis*) was the third largest woodpecker in the world. It is believed that the IBW went extinct in the middle of the twentieth century. To illustrate the use of our model when there are both certain and uncertain sightings, we analyzed the sighting record of the IBW given in Elphick *et al.* (2010). The same sighting data was used in Solow *et al.* (2012) and Solow & Beet (2014) to infer extinction about IBW. However, these approaches assumed that the certain sightings, valid uncertain sightings and invalid uncertain sightings follow independent stationary Poisson processes with constant rates. We relax this assumption and suppose the sightings could evolve according to a non-homogeneous Poisson process. Similar to Solow & Beet (2014), we assume that all sightings based on physical evidence are certain, and all sightings that are not based on physical evidence are uncertain.

Table 2: Summary of the posterior distribution of τ_E for IBW

	95% HDI Low	median	95% HDI High
$\tau_E \vert S$	1939	1950	1956

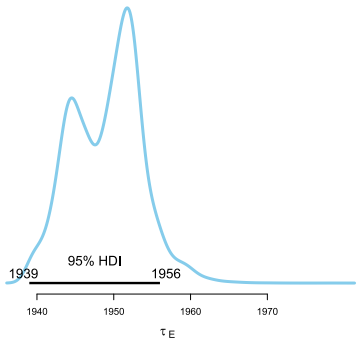

Figure 3: Posterior distribution plot of τ_E for the IBW. Black solid line above x-axis shows the 95% HDI for the posterior distribution.

The posterior distribution of τ_E is plotted in Fig. 3 and the 95% HDI for the posterior extinction year is given in Table 2. According to Table 2, the median extinction year is 1950 with a 95% upper bound in 1956. Also, the extinction time τ_E is a bimodal distribution (see Fig. 3), where the modes are approximately located at 1944 and 1952. In the next paragraphs we explain the reason for this bimodal result.

In the model, extinction time was formulated as a termination point for certain sightings and a change-point for uncertain sightings (see Fig. 1). Hence, the inference about extinction time is significantly influenced by the last certain sighting and by any rate change in the uncertain sightings. For IBW, the first mode (1994) is associated with the last certain sighting while the second mode (1952) arises due to the change point of the uncertain sighting. According to Fig. 4, the first mode in year 1994 is closer to the last certain sighting in 1939. The sudden ending of certain sightings at this year indicate its possible influence over extinction time. On the other hand, the second mode in 1952 is another possible change point as the rate of uncertain sightings increased until 1952 and then changed its behaviour afterwards. Thus, 1952 becomes another possible candidate for extinction time.

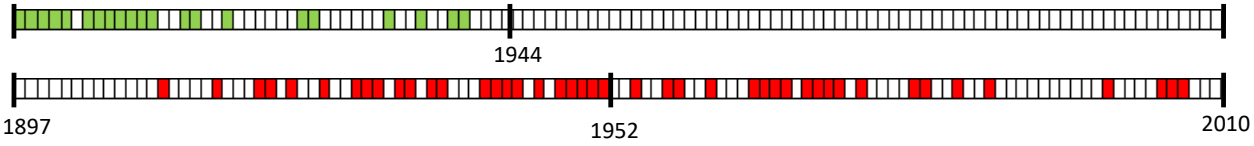

Figure 4: Graphical representation of IBW certain sightings and uncertain sightings. Green represents the years where there are certain sightings while red represents the years of uncertain sightings.

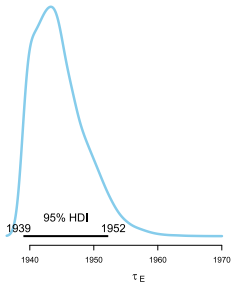

Figure 5: Posterior distribution plot of τ_E for the IBW with change-point and homogeneous rate assumptions. Black solid line above x-axis shows the 95% HDI for τ_E.

In order to further investigate the bimodal behaviour, the IBW sighting record was modelled using a homogeneous Poisson process for uncertain and certain sightings. The model can be obtained by allowing $\alpha_c = \alpha_{u1} = \alpha_{u2} = 1$ in Equation 9. As seen in Fig. 5, when the rate of certain and uncertain sightings are assumed to have a constant sighting rate, while allowing for a change-point in uncertain sightings, the posterior distribution for τ_E is unimodal with its mode being closer to the first mode in Fig. 3. This results indicates that the bimodal distribution in Fig. 3 is a result of the heterogeneous rate assumption in uncertain sightings.

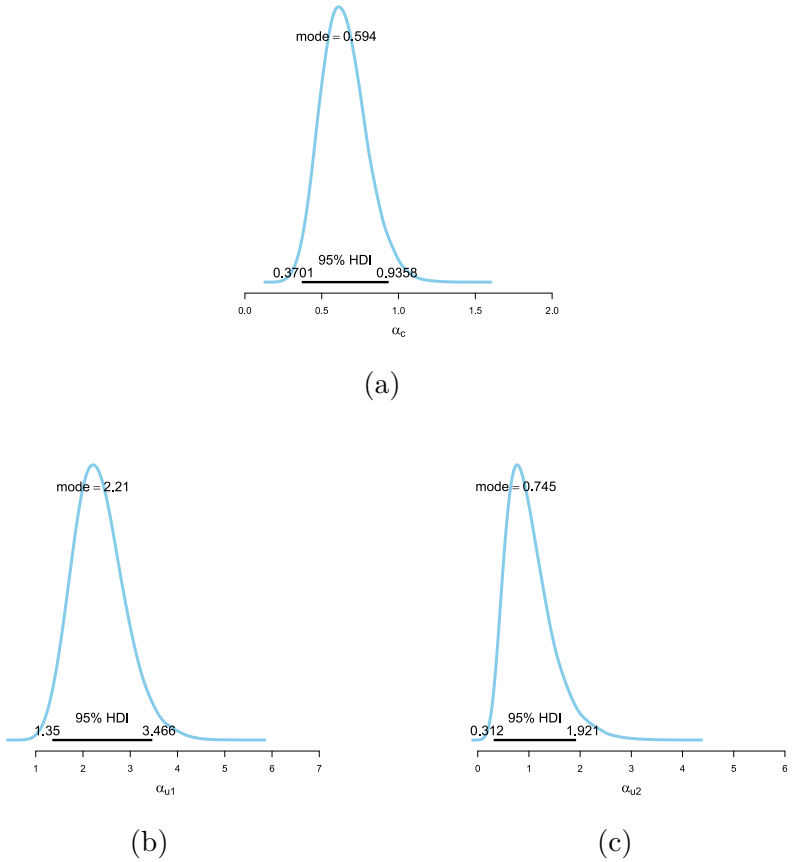

Figure 6: Posterior distribution plots for the model parameters α_c, α_{u1} and α_{u2} for IBW. Black solid line above x-axis shows the 95% HDI for the posterior distribution. (A) Posterior distribution of α_c. (B) Posterior distribution of α_{u1}. (C) Posterior distribution of α_{u2}.

Other model parameters of interest are the shape parameters α_c, α_{u1} and α_{u2}, which reflect if and how the sighting rates change over time. Fig. 6a shows that the 95% HDI for α_c is (0.37, 0.94). Thus, the null hypothesis that $\alpha_c \geq 1$ can be rejected, or in other words we can be 95% confidence that α_c is less than 1. This implies that the certain sighting rate declined over the pre-extinction period for IBW. Similar inferences can be made on α_{u1} and α_{u2}. The 95% HDI for α_{u1} and α_{u2} are (1.35,3.46) and (0.31, 1.92), respectively (see Fig. 6b and Fig. 6c). Since the lower bound of α_{u1} is greater than 1, the uncertain sighting rate before extinction (i.e. τ_E) increased over time. In contrast, the 95% HDI for α_{u2} contains 1 inside its interval, and thus implies a constant (invalid) sighting rate after extinction for IBW.

Using Fig. 7, let us now examine the impact of model assumptions on the cumulative

posterior extinction probability.

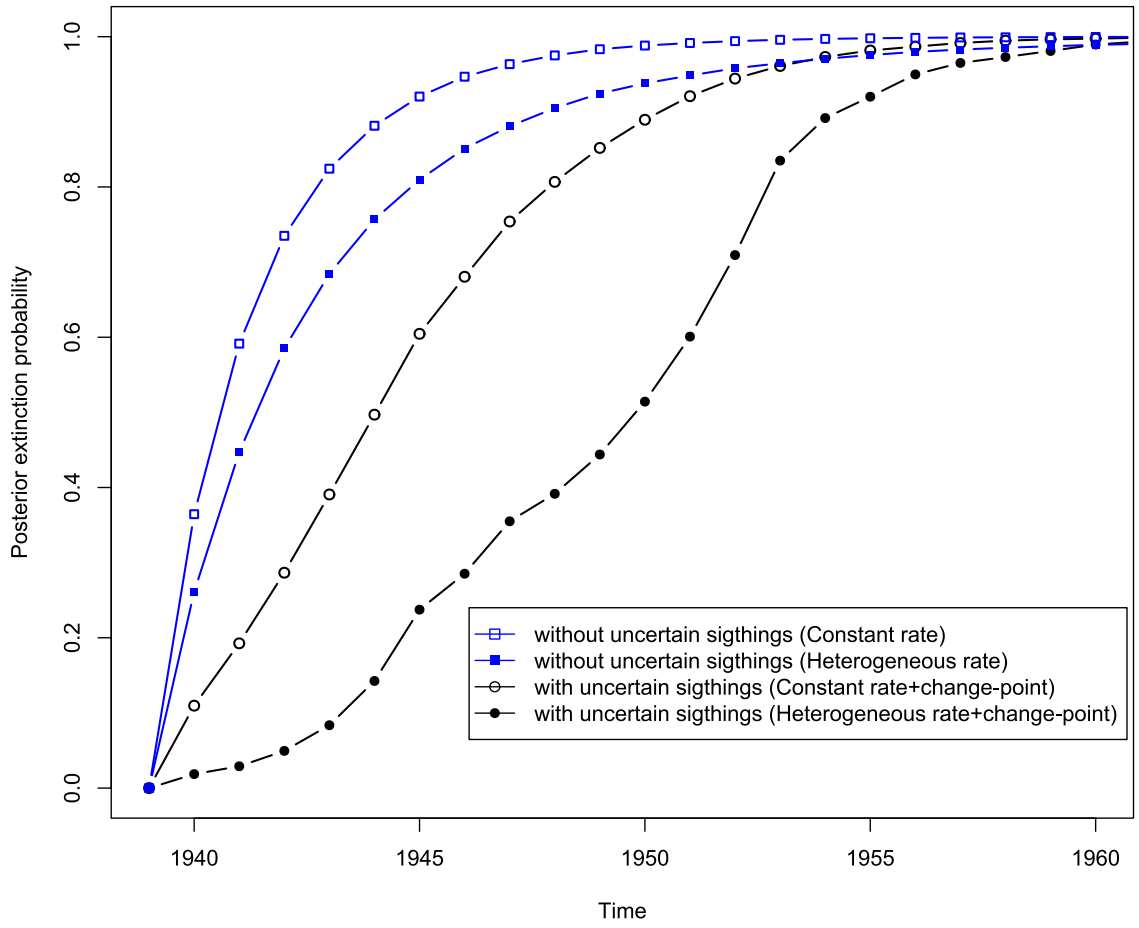

Figure 7: Time series plot of the posterior extinction probability under different assumptions for the IBW.

The cumulative posterior extinction probability evaluated at a considered year (say t_i) is the area under the posterior distribution of τ_E from zero to t_i in Fig. 3 (for the case of uncertain sightings). Through Fig. 7 we can discuss the importance of model assumptions as well as the uncertain sightings on the posterior extinction probability. For instance, let us assume that ecologists are interested in inferring whether the IBW was extinct by a given year, say 1948. In such a situation, if one uses only certain sightings with a constant sighting rate assumption, then the posterior extinction probability for IBW by 1948 is 0.97 (i.e., $P(\tau_E \leq 1948|D_c, \alpha_c = 1) = 0.97$). But if the uncertain sightings were included with a constant rate assumption then the probability is reduced to 0.75 (i.e., $P(\tau_E \leq 1948|D_c, D_u, \alpha_c =$

$1, \alpha_{u1} = 1, \alpha_{u2} = 1) = 0.75$). In the latter case, the analysis indicates that the inclusion of uncertain sightings still favours extinction but with a lower probability than before. The same probability is further reduced to 0.38 when the constant rate assumption is relaxed by allowing the process to be non-homogeneous (i.e., $P(\tau_E \leq 1948|D_c, D_u) = 0.38$). Under this scenario the extinction of IBW by 1948 is questionable. Through this simple example it is clear how each model assumption will produce different posterior extinction probabilities.

4 Discussion

In this paper, the work of Solow & Beet (2014) was extended for predicting extinction when the sightings, both certain and uncertain, follow non-homogeneous Poisson processes. It was assumed that certain and uncertain sightings evolve according to two independent non-homogeneous Poisson processes between $(0, \tau)$. Over the period (τ, T), the uncertain sightings follow a different non-homogeneous Poisson process. The new approach can be used to test if the sighting rates for certain and uncertain sightings were decreasing, increasing or constant over the studied time period.

The model was applied on two real-world case studies covering a certain sighting only scenario (the black-footed ferret), and a case where both certain and uncertain sightings appear in the sighting record (the IBW). The null hypothesis that the black-footed ferret and the IBW is extant by the sighting end period (i.e 1990 and 2010) was rejected and our statistical analysis suggests that the black-footed ferret and the IBW went extinct in the 1980s and 1950s, respectively. In addition to these conclusions, the posterior distributions of α_c suggested that both these species had a declining certain sighting rate pre-extinction, possibly due to decline in the population as the species reach extinction. The uncertain sighting rate, however, indicated an increase before extinction for IBW which probably reflects the media and ecological attention received (U.S. Fish and Wildlife Service 2010).

The main advantage of the method described in this paper is that it does not have any underlying assumptions on the sighting rates. Through Fig. 7, we demonstrate the impact of these assumption on the posterior extinction probability using IBW sighting data. For example, if one assumes a constant sighting rate for both certain and uncertain sightings, then the cumulative posterior extinction probability is over estimated as shown in Fig. 7. In contrast if the true certain sighting rate was increasing before extinction then assuming a constant rate would under-estimate the true extinction probability. Hence the inferences made under constant rate assumption will be inaccurate if the true underlying rate is heterogeneous.

Data accessibility. IBW sighting data used in this article are available at https://doi.org/10.5281/zenodo.3766207.

Competing interests. We declare we have no competing interests.

Authors' contributions. L.S., H.D. and Y.W. secured funding. S.K. contributed to the concept and designed the article content while consulting other authors. S.K. conducted the analyses and wrote the initial draft of the manuscript. All authors revised the manuscript and gave final approval for publication.

Funding. This work was funded by Australian Research Council[Grant number: DP 150102472].

References

Achcar, J.A., Rodrigues, E.R., Paulino, C.D. & Soares, P. (2010) Non-homogeneous poisson models with a change-point: an application to ozone peaks in mexico city. *Environmental and Ecological Statistics*, **17**, 521–541.

Barnosky, A.D., Matzke, N., Tomiya, S., Wogan, G.O., Swartz, B., Quental, T.B., Marshall, C., McGuire, J.L., Lindsey, E.L., Maguire, K.C. *et al.* (2011) Has the earth's sixth mass extinction already arrived? *Nature*, **471**, 51–57.

Boakes, E.H., Rout, T.M. & Collen, B. (2015) Inferring species extinction: The use of sighting records. *Methods in Ecology and Evolution*, **6**, 678–687.

Ceballos, G., García, A. & Ehrlich, P.R. (2010) The sixth extinction crisis: Loss of animal populations and species. *Journal of Cosmology*, **8**, 31.

Daily, G.C. & Matson, P.A. (2008) Ecosystem services: From theory to implementation. *Proceedings of the National Academy of Sciences*, **105**, 9455–9456.

Dirzo, R. & Raven, P.H. (2003) Global state of biodiversity and loss. *Annual Review of Environment and Resources*, **28**.

Dobson, A. & Lyles, A. (2000) Black-footed ferret recovery. *Science*, **288**, 985–988.

Ehrlich, P.R. & Ehrlich, A.H. (2013) Can a collapse of global civilization be avoided? *Proceedings of the Royal Society B: Biological Sciences*, **280**, 20122845.

Elphick, C.S., Roberts, D.L. & Reed, J.M. (2010) Estimated dates of recent extinctions for north american and hawaiian birds. *Biological Conservation*, **143**, 617–624.

Guarnaccia, C., Quartieri, J., Tepedino, C. & Rodrigues, E.R. (2015) An analysis of airport noise data using a non-homogeneous poisson model with a change-point. *Applied Acoustics*, **91**, 33–39.

Hall, P., Wang, J.Z. *et al.* (1999) Estimating the end-point of a probability distribution using minimum-distance methods. *Bernoulli*, **5**, 177–189.

Ho, C.H. (1991) Nonhomogeneous poisson model for volcanic eruptions. *Mathematical Geology*, **23**, 167–173.

Jarić, I. & Ebenhard, T. (2010) A method for inferring extinction based on sighting records that change in frequency over time. *Wildlife Biology*, **16**, 267–275.

Kodikara, S., Demirhan, H., Wang, Y. & Stone, L. (2020) Inferring extinction date of a species using non-homogeneous poisson processes with a change-point. *Methods in Ecology and Evolution*.

Lee, T.E., Bowman, C. & Roberts, D.L. (2017) Are extinction opinions extinct? *PeerJ*, **5**, e3663.

Lee, T.E., McCarthy, M.A., Wintle, B.A., Bode, M., Roberts, D.L. & Burgman, M.A. (2014) Inferring extinctions from sighting records of variable reliability. *Journal of Applied Ecology*, **51**, 251–258.

Mace, G.M., Norris, K. & Fitter, A.H. (2012) Biodiversity and ecosystem services: A multilayered relationship. *Trends in Ecology & Evolution*, **27**, 19–26.

Rao, C.R., Rao, C. & Govindaraju, V. (2006) *Handbook of statistics*. Elsevier.

Rigdon, S.E. & Basu, A.P. (1989) The power law process: a model for the reliability of repairable systems. *Journal of Quality Technology*, **21**, 251–260.

Roberts, D.L. & Solow, A.R. (2003) Flightless birds: when did the dodo become extinct? *Nature*, **426**, 245.

Smith, R.L. & Weissman, I. (1985) Maximum likelihood estimation of the lower tail of a probability distribution. *Journal of the Royal Statistical Society: Series B (Methodological)*, **47**, 285–298.

Solow, A., Smith, W., Burgman, M., Rout, T., Wintle, B. & Roberts, D. (2012) Uncertain sightings and the extinction of the ivory-billed woodpecker. *Conservation Biology*, **26**, 180–184.

Solow, A.R. (1993) Inferring extinction in a declining population. *Journal of Mathematical Biology*, **32**, 79–82.

Solow, A.R. (2005) Inferring extinction from a sighting record. *Mathematical Biosciences*, **195**, 47–55.

Solow, A.R. & Beet, A.R. (2014) On uncertain sightings and inference about extinction. *Conservation biology*, **28**, 1119–1123.

U.S. Fish and Wildlife Service (2010) *Recovery plan for the Ivory-billed woodpecker (Campephilus principalis)*. US Fish and Wildlife Service, Southeast Region.

Wisely, S.M., Santymire, R.M., Livieri, T.M., Mueting, S.A. & Howard, J. (2008) Genotypic and phenotypic consequences of reintroduction history in the black-footed ferret (mustela nigripes). *Conservation Genetics*, **9**, 389–399.